COMMUN. MATH. SCI.
Vol. 14, No. 6, pp. 1517–1534

ON THE MAXIMUM PRINCIPLE PRESERVING SCHEMES FOR THE GENERALIZED ALLEN–CAHN EQUATION*

JIE SHEN†, TAO TANG‡, AND JIANG YANG§

Abstract. This paper is concerned with the generalized Allen–Cahn equation with a nonlinear mobility that may be degenerate, which also includes an advection term appearing in many phase-field models for multi-component fluid flows. A class of maximum principle preserving schemes will be studied for the generalized Allen–Cahn equation, with either the commonly used polynomial free energy or the logarithmic free energy, and with a nonlinear degenerate mobility. For time discretization, the standard semi-implicit scheme as well as the stabilized semi-implicit scheme will be adopted, while for space discretization, the central finite difference is used for approximating the diffusion term and the upwind scheme is employed for the advection term. We establish the maximum principle for both semi-discrete (in time) and fully discretized schemes. We also provide an error estimate by using the established maximum principle which plays a key role in the analysis. Several numerical experiments are carried out to verify our theoretical results.

Key words. Allen–Cahn equation, stability, error estimate, maximum principle, finite difference.

AMS subject classifications. 65M06, 65M12, 65G20.

1. Introduction

In this paper, we study the numerical approximation of the generalized Allen–Cahn equation

$$\frac{\partial u}{\partial t}+\boldsymbol{v}\cdot\nabla u=M(u)\left(\epsilon\Delta u-\frac{1}{\epsilon}F'(u)\right),\quad \mathbf{x}\in\Omega,\ t\in(0,T], \tag{1.1}$$

$$u(\mathbf{x},0)=u_0(\mathbf{x}),\quad \mathbf{x}\in\bar{\Omega}, \tag{1.2}$$

subjected to suitable boundary conditions such as periodic boundary conditions, homogeneous Neumann boundary conditions, or homogeneous Dirichlet boundary conditions. In (1.1), Ω is a bounded domain in R^d ($d=1,2,3$), $M(u)$ is a nonnegative mobility functional, $F(u)$ is a double-well potential, and $\boldsymbol{v}(\cdot,t)$ is a given velocity field.

The Allen–Cahn equation was originally introduced by Allen and Cahn in [1] to describe the motion of anti-phase boundaries in crystalline solids. Recently, the Allen–Cahn equation has been widely used to model various phenomena, e.g., mean curvature flow [8,13], image segmentation [2], and many problems in materials science. In particular, it has become a basic model equation for the diffuse interface approach developed to study phase transitions and interfacial dynamics in materials science, see, e.g., [14, 16], in which a velocity field is involved in the Allen–Cahn phase equation. This is one of our

*Received: October 10, 2015; accepted (in revised form): November 29, 2015. Communicated by Chun Liu.

†Department of Mathematics, Purdue University, West Lafayette, IN 47907, USA (shen@math.purdue.edu).

The work of J.S. was partially supported by NSF grant DMS-1419053 and AFOSR grant FA9550-16-1-0102.

‡Department of Mathematics, South University of Science and Technology, Shenzhen 518055, Guangdong, P.R. China and Department of Mathematics & Institute for Computational and Theoretical Studies, Hong Kong Baptist University, Kowloon Tong, Hong Kong (ttang@hkbu.edu.hk).

The work of T.T. was partially supported by Hong Kong Research Grants Council CERG grants, National Science Foundation of China, and Hong Kong Baptist University FRG grants.

§Department of Applied Physics and Applied Mathematics, Columbia University, New York, NY10027, USA (jyanghkbu@gmail.com).

motivations to study this generalized model. Another motivation is that the nonlinear degenerate mobility can more accurately describe the physics of phase separation, as pure phases must have vanishing mobility, (see [12,18]).

Compared with the simple version of Allen–Cahn equation [1], the generalized Allen–Cahn equation (1.1) is more complex due to the added velocity field and the nonlinear mobility. However, the generalized Allen–Cahn equations still preserve two intrinsic properties as ones of the simple version, i.e., nonlinear energy stability and maximum principle, which will be described in more detail below.

Consider the energy functional of (1.1) with periodic boundary conditions, homogeneous Neumann boundary conditions, or homogeneous Dirichlet boundary conditions

$$E(u)=\int_\Omega\left(\frac{1}{2}\epsilon|\nabla u|^2+\frac{1}{\epsilon}F(u)\right)dx. \tag{1.3}$$

As an L^2-gradient flow, E is a decreasing function of time in the sense of

$$\frac{dE(u(t))}{dt}=-\int_\Omega\left(M(u)\left|\epsilon\Delta u-\frac{1}{\epsilon}F'(u)\right|^2\right)\le 0. \tag{1.4}$$

This is often called the nonlinear energy stability. We shall assume that the free energy functional $F(u)$ in (1.1) has a double well form with minima at β and $-\beta$, where β satisfies

$$F'(\beta)=F'(-\beta)=0, \tag{1.5}$$

and $F'(u)$ satisfies the monotone conditions away from $(-\beta,\beta)$:

$$F'(u)<0,\ \forall u\in(-\infty,-\beta);\quad F'(u)>0,\ \forall u\in(\beta,\infty). \tag{1.6}$$

The mobility function is assumed to be nonnegative, i.e.,

$$M(u)\ge 0,\quad \forall u\in(-\infty,\infty). \tag{1.7}$$

Under the conditions (1.5)-(1.7), as a typical nonlinear reaction-diffusion-advection equation, it can be shown that the generalized Allen–Cahn equation (1.1) satisfies a maximum principle: if the initial value and the boundary conditions are bounded by constant β given in (1.5), then the entire solution is also bounded by β, i.e.,

$$\|u(\cdot,t)\|_\infty\le\beta,\quad \forall t>0. \tag{1.8}$$

This is called maximum principle for (1.1).

As exact solutions of these phase-field models are not readily available, numerical methods play an important role in the study of these models. The idea of designing numerical techniques that satisfy the nonlinear energy stability for the Allen–Cahn equation and more general phase field models has been extensively studied in the past decades. The first study was carried out by Du and Nicolaides [5] who derived a second-order accurate unconditionally stable time-stepping scheme for the Cahn–Hilliard equation. Elliott and Stuart [6] (see also [7]) derived an unconditionally nonlinear energy-stable time-stepping scheme, based on a convex splitting, for a class of semi linear parabolic equations. On the other hand, it is even more important, and more difficult, to study the energy stability for fully discrete schemes. For the Allen–Cahn equation, some recent stability analysis can be found in [9–11, 15, 19, 20]. Very recently,

a stronger stability in L^∞-norm, i.e., the maximum principle, is established for fully discrete schemes of the simplified version of the Allen–Cahn equation [17].

In this paper, we will mainly focus on establishing the maximum principle for finite difference approximations to the generalized Allen–Cahn Equation (1.1) with potential satisfying (1.5)-(1.6) and mobility satisfying (1.7). Two types of potential $F(u)$ will be considered in this paper:

the polynomial potential:

$$F(u)=\frac{1}{4}(u^2-1)^2, \tag{1.9}$$

the logarithmic free energy function:

$$F(u)=\frac{\theta}{2}[(1+u)\ln(1+u)+(1-u)\ln(1-u)]-\frac{\theta_c}{2}u^2, \tag{1.10}$$

where θ,θ_c are two positive constants. More details about the latter one can be found in [3, 4]. We emphasize that the numerical maximum principle is very important in the approximations of the generalized Equation ((1.1), especially for the logarithmic free energy and nonlinear degenerate mobility. Note that if numerical maximum is not satisfied then complex values will occur in the numerical solutions due to the logarithm arithmetic, and the nonlinear mobility function may become negative.

The rest of this paper is organized as follows. In Section 2, we prove that the semi-discretized scheme for (1.1) can preserve the maximum principle. In Section 3, we establish the numerical maximum principle for the fully discretized scheme with semi-implicit time discretization and, central finite deference for the diffusion term and upwind scheme for the advection term. In Section 4, the polynomial and the logarithmic form of energies are studied, and in Section 5 the error estimate is given using the established numerical maximum principle. Several numerical experiments are carried out to verify our theoretical results in Section 6. Moreover, an adaptive algorithm based on the stabilized scheme is adopted for long time simulations, which is found robust and efficient. Some concluding remarks are given in the final section.

2. The semi-discrete scheme

First, we consider the standard linearized semi-implicit scheme

$$\frac{u^{n+1}-u^n}{\tau}+\boldsymbol{v}^{n+1}\cdot\nabla u^{n+1}=M(u^n)\left(\epsilon\Delta u^{n+1}-\frac{1}{\epsilon}F'(u^n)\right), \tag{2.1}$$

which can be rewritten as

$$u^{n+1}+\tau\boldsymbol{v}^{n+1}\cdot\nabla u^{n+1}-\tau\epsilon M(u^n)\Delta u^{n+1}=u^n-\frac{\tau}{\epsilon}M(u^n)F'(u^n), \tag{2.2}$$

where $u^n,\boldsymbol{v}^n$ are approximations of $u(x,t_n),\boldsymbol{v}(x,t_n)$ respectively, and τ is the time step.

To begin with, we estimate the right-hand side of the above equality in the following lemma.

LEMMA 2.1. *Denote*

$$f(x)=x-\frac{\tau}{\epsilon}M(x)F'(x);\quad x\in[-\beta,\beta], \tag{2.3}$$

where $F'(x)$ satisfies (1.5) *and* (1.6). *Then, we have*

$$\max_{|x|\le\beta}f(x)=f(\beta)=\beta;\quad \min_{|x|\le\beta}f(x)=f(-\beta)=-\beta, \tag{2.4}$$

under the condition

$$\tau \max_{x\in[-\beta,\beta]} (M'(x)F'(x)+M(x)F''(x)) \le \epsilon. \tag{2.5}$$

Proof. It follows from (1.5) that $f(\beta)=\beta$, $f(-\beta)=-\beta$. It is sufficient to show that $f'(x)\ge 0$ holds in $[-\beta,\beta]$, which is true by observing

$$f'(x)=1-\frac{\tau}{\epsilon}(M'(x)F'(x)+M(x)F''(x)), \tag{2.6}$$

and using the condition (2.5). ∎

We use $\|\cdot\|_\infty$ to denote the standard infinity norm for a function, a vector or a matrix.

THEOREM 2.2. *Assume the initial value satisfies*

$$\|u_0\|_\infty \le \beta, \tag{2.7}$$

and the time step size τ satisfies the condition (2.5)*. Then the scheme* (2.1)*, with periodic boundary conditions, homogeneous Neumann boundary conditions, or homogeneous Dirichlet boundary conditions, preserves the maximum principle, i.e.,*

$$\|u^n\|_\infty \le \beta, \quad \text{for all } n\ge 0. \tag{2.8}$$

Proof. We proceed by induction. By assumption, the result is true for $n=0$. Assume the result holds for $n\le m$ i.e. $\|u^m\|_\infty \le \beta$. Next we check this holds for $n=m+1$. By (2.2) and the definition of $f(x)$, we get

$$u^{m+1}+\tau \boldsymbol{v}\cdot\nabla u^{m+1}-\tau\epsilon M(u^m)\Delta u^{m+1}=f(u^m). \tag{2.9}$$

By Lemma 2.1 and $\|u^m\|_\infty \le \beta$, we find

$$\|f(u^m)\|_\infty \le \beta. \tag{2.10}$$

Assume the solution u^{m+1} of (2.9) achieves the maximum at x^* inside Ω, thus

$$\nabla u^{m+1}(x^*)=\mathbf{0},\ \Delta u^{m+1}(x^*)\le 0. \tag{2.11}$$

Consequently,

$$\max(u^{m+1}) \le f(u^m(x^*)). \tag{2.12}$$

Similarly, if the solution achieves the minimum at x^{**} inside Ω, we have

$$\min(u^{m+1}) \ge f(u^m(x^{**})). \tag{2.13}$$

Since the boundary values are bounded by β, we find

$$\|u^{m+1}\|_\infty \le \|f(u^m)\|_\infty \le \beta. \tag{2.14}$$

This completes the proof of the induction. ∎

We observe that the time step constraint (2.5) can be very severe when $\epsilon \ll 1$. To reduce the time step restriction, we consider the stabilized scheme (cf. [15])

$$\frac{u^{n+1}-u^n}{\tau}+\boldsymbol{v}^{n+1}\cdot\nabla u^{n+1}+S(u^{n+1}-u^n)=M(u^n)\left(\epsilon\Delta u^{n+1}-\frac{1}{\epsilon}F'(u^n)\right), \tag{2.15}$$

where $S \geq 0$ is a stabilizing parameter to be determined.

COROLLARY 2.3. *Under the same initial values and boundary conditions in Theorem 2.2, if the time step size τ satisfies the following condition*

$$\frac{1}{\tau} + S \geq \frac{1}{\epsilon} \max_{x \in [-\beta,\beta]} (M'(x)F'(x) + M(x)F''(x)). \tag{2.16}$$

the stabilized scheme (2.15) *preserves the maximum principle, i.e.,*

$$\|u^n\|_\infty \leq \beta, \quad \text{for all } n \geq 0. \tag{2.17}$$

The proof is similar to that of Theorem 2.2, so we will omit it here. In following sections, we also omit the proof for the stabilized schemes as their proof is similar to that for the non-stabilized ones.

3. The fully discretized semi-implicit scheme

In this section, we construct fully discrete semi-implicit schemes with finite differences for the spatial variable. For simplicity, we assume that Ω is a rectangular domain with homogeneous Dirichlet boundary conditions, although the proof techniques are valid for periodic and homogeneous Neumann boundary conditions.

3.1. 1D case. First, we handle the diffusion term by the central finite difference method

$$u_{xx}(x_i,\cdot) \approx \frac{u_{i-1} - 2u_i + u_{i+1}}{h^2}. \tag{3.1}$$

We denote the differential matrix D_h as the discrete matrix of the Laplace Operator. The differential matrix D_h with Dirichlet boundary conditions on interval $[0, L]$ in 1D is given by

$$D_h = \frac{1}{h^2} \begin{bmatrix} -2 & 1 & & & \\ 1 & -2 & 1 & & \\ & \ddots & \ddots & \ddots & \\ & & 1 & -2 & 1 \\ & & & 1 & -2 \end{bmatrix}_{N \times N},$$

where $h = L/(N+1)$ is the mesh size. Then we handle the advection term by the upwind scheme

$$au_x = a^+ u_i^- + a^- u_i^+, \tag{3.2}$$

where a^+ and a^- are defined as

$$a^+ = \max\{0, a\}, \quad a^- = \min\{0, a\}, \tag{3.3}$$

and u_i^- and u_i^+ are defined as

$$u_i^- = \frac{-u_{i-1} + u_i}{h}, \quad u_i^+ = \frac{u_{i+1} - u_i}{h}. \tag{3.4}$$

Let us denote

$$\Lambda_1^{n+1} = \mathrm{diag}(\mathrm{abs}(V^{n+1})), \quad \Lambda_2^n = \mathrm{diag}(M(U^n)), \tag{3.5}$$

where V is a vector, $\mathrm{diag}(V)$ is the diagonal matrix with diagonal elements being components of V,

$$\mathrm{abs}(V^{n+1}) = (|v_1^{n+1}|,\dots,|v_N^{n+1}|)^T, \quad M(U^n) = (M(u_1^n),\dots,M(u_N^n))^T,$$

and

$$A_v = \frac{1}{2h}\begin{bmatrix} -2 & 1-\mathrm{sign}(v_1^{n+1}) & & & \\ 1+\mathrm{sign}(v_2^{n+1}) & -2 & 1-\mathrm{sign}(v_2^{n+1}) & & \\ & \ddots & \ddots & \ddots & \\ & & 1+\mathrm{sign}(v_{N-1}^{n+1}) & -2 & 1-\mathrm{sign}(v_{N-1}^{n+1}) \\ & & & 1+\mathrm{sign}(v_N^{n+1}) & -2 \end{bmatrix}_{N\times N}.$$

We consider the fully discrete version of the semi-discrete scheme (2.2)

$$U^{n+1} - \tau\Lambda_1^{n+1}A_vU^{n+1} - \tau\epsilon\Lambda_2^n D_hU^{n+1} = f(U^n), \tag{3.6}$$

and the fully discrete version of the stabilized scheme (2.15)

$$U^{n+1} + S\tau U^{n+1} - \tau\Lambda_1^{n+1}A_vU^{n+1} - \tau\epsilon\Lambda_2^n D_hU^{n+1} = f(U^n) + S\tau U^n. \tag{3.7}$$

where U^n represents the vector of numerical solution and $f(U^n) = (f(U_1^n),\dots,f(U_N^n))^T$, and $-\Lambda_1^{n+1}A_v$ represents the differential matrix for the advection term.

We first prove a useful lemma.

LEMMA 3.1. *Let $B = (b_{ij}) \in R^{N\times N}$ and $A = aI - B$, where $a > 0$. If B is a negative diagonally dominant (NDD) matrix, i.e.*

$$b_{ii} \le 0 \quad \textit{and} \quad b_{ii} + \sum_{j\neq i}|b_{ij}| \le 0,\ \forall i, \tag{3.8}$$

then, A is invertible and its inverse satisfies

$$\|A^{-1}\|_\infty \le \frac{1}{a}. \tag{3.9}$$

Proof. Since A is diagonally dominant, A is invertible. If B is a zero matrix, the conclusion obviously holds. Otherwise, we denote

$$b = \max_i(-b_{ii}) > 0. \tag{3.10}$$

Then we rewrite A as

$$A = (a+b)I - (bI+B) := (a+b)(I - sC), \tag{3.11}$$

where $s = \frac{b}{a+b} < 1$ and matrix $C = I + \frac{1}{b}B := (c_{ij})$. Thus

$$\begin{aligned}\|C\|_\infty &= \max_i \sum_j |c_{ij}| = \max_i \left(|1 + \frac{b_{ii}}{b}| + \frac{1}{b}\sum_{j\neq i}|b_{ij}| \right) \\ &= \max_i \left(1 + \frac{1}{b}(b_{ii} + \sum_{j\neq i}|b_{ij}|) \right) \le 1. \end{aligned} \tag{3.12}$$

Then we have

$$\rho(sC) = s\rho(C) \le s < 1, \tag{3.13}$$

where $\rho(C)$ is the spectral radius of matrix C. As the inverse of $I - sC$ can be represented by the power series of sC, we have

$$\|A^{-1}\|_\infty = \Big|\Big| \frac{1}{a+b} \sum_{p=0}^{\infty} (sC)^p \Big|\Big|_\infty \le \frac{1}{a+b} \sum_{p=0}^{\infty} s^p \|C\|_\infty^p \le \frac{1}{a+b} \cdot \frac{1}{1-s} = \frac{1}{a}, \tag{3.14}$$

where in the last step we have used the definition $s = \frac{b}{a+b} < 1$. ∎

THEOREM 3.2. *Assume that* $\max_{\boldsymbol{x}\in\bar{\Omega}} |u_0(\boldsymbol{x})| \le \beta$. *Then*

- *the fully discrete scheme* (3.6) *preserves the maximum principle in the sense that* $\|U^n\|_\infty \le \beta$, *provided that the condition* (2.5) *is satisfied;*
- *the stabilized fully discrete scheme* (3.7) *preserves the maximum principle in the sense that* $\|U^n\|_\infty \le \beta$ *provided that the condition* (2.16) *is satisfied.*

Proof. We proceed by induction. Obviously, $\|U^0\|_\infty \le \max|u_0(\mathbf{x})| \le \beta$. We assume the result holds for $n \le m$ i.e. $\|U^m\|_\infty \le \beta$. Next we check this holds for $n = m+1$. First, we denote

$$G^n = \tau \Lambda_1^{n+1} A_v + \tau\epsilon \Lambda_2^n D_h. \tag{3.15}$$

Since both A_v and D_h are NDD matrices together with the nonnegative property of Λ_1^{n+1} and Λ_2^n, it is easy to verify that G^n is an NDD matrix. With G^n the linear scheme (3.6) can be simply rewritten as

$$U^{m+1} = (I - G^m)^{-1} f(U^m). \tag{3.16}$$

It follows from Lemma 2.1 and $\|U^m\|_\infty \le \beta$ that

$$\|f(U^m)\|_\infty \le \beta. \tag{3.17}$$

As G^m is NDD, using Lemma 3.1 gives

$$\|(I - G^m)^{-1}\|_\infty \le 1. \tag{3.18}$$

Consequently,

$$\|U^{m+1}\|_\infty \le \|(I - G^m)^{-1}\|_\infty \|f(U^m)\|_\infty \le \beta. \tag{3.19}$$

The result for the stabilized scheme (3.7) can be established in a similar fashion. ∎

REMARK 3.3. Since we have established the maximum principle for both semi-discrete scheme (2.1) and the fully discrete scheme (3.6), $M(u^n)$, and Λ_2^n are always nonnegative, both schemes (2.1) and (3.6) are in fact linear elliptic equations with variable coefficients, for which unique solvability can be easily established.

3.2. Extension to multi-dimensional case. For brevity, we just outline the main ideas for extending the results to the multi-dimensional rectangular domains.

We can see that the analysis in the 1D case focuses on obtaining the L^∞ estimate for the solution to one linear system. We achieve it by two steps: the L^∞ norm of the system matrix $I-G$ and the L^∞ norm of the right-hand side $f(U^m)$. For multi-dimensional rectangular domains, the estimate for the right-hand side is exactly the same as the 1D case since we accomplish it point-wisely. If we also use central finite difference method to handle the diffusion term and upwind scheme to handle the advection term, we can still ensure that the stiffness matrix is NDD. Consequently, the L^∞ norm of the stiffness matrix for the multi-dimensional case can be bounded in the same way as in the 1D case. In summary, the conditions to guarantee the maximum principle for the multi-dimensional case should be same as in the 1D case.

4. Polynomial free energy and logarithmic free energy

The results in the last two sections were derived with the general conditions (1.5)–(1.6) for the potential function $F(u)$ and (1.7) for the mobility function $M(u)$. In this section, we apply the previous results to two cases commonly used in practice.

4.1. Polynomial free energy with constant mobility. We consider, as the first example, the Allen–Cahn equation in its simplest form: the mobility $M(u)=1$ and

$$F(u)=\frac{1}{4}(u^2-1)^2, \quad F'(u)=u^3-u. \tag{4.1}$$

In this case, is is easy to show that (1.5)–(1.6) are satisfied with $\beta=1$.

A direct consequence of Theorem 2 is the following:

COROLLARY 4.1. *Assume* $\max_{\boldsymbol{x}\in\bar{\Omega}}|u_0(\boldsymbol{x})|\le 1$. *Then, the fully discrete scheme* (3.6) *with* $M(u)=1$ *and* $F(u)=\frac{1}{4}(u^2-1)^2$ *preserves the maximum principle in the sense that* $\|U^n\|_\infty\le 1$ *for all* $n\ge 0$, *provided that*

$$0<\tau\le\frac{\epsilon}{2}; \tag{4.2}$$

and the stabilized fully discrete scheme (3.7) *also preserves the maximum principle in the sense that* $\|U^n\|_\infty\le 1$ *for all* $n\ge 0$, *provided that*

$$\frac{1}{\tau}+S\ge\frac{2}{\epsilon}. \tag{4.3}$$

We note that the above result for (3.6) without the convective term was proved in [17].

4.2. Logarithmic free energy with nonlinear degenerate mobility. We now consider a more complicated situation with a logarithmic free energy functional

$$F(u)=\frac{\theta}{2}[(1+u)\ln(1+u)+(1-u)\ln(1-u)]-\frac{\theta_c}{2}u^2, \tag{4.4}$$

where $\theta<\theta_c$ are two positive constants, and a degenerated nonlinear mobility

$$M(u)=D(1-u^2), \tag{4.5}$$

which D is a positive constant. In this case, we have

$$F'(u)=\frac{\theta}{2}\ln\left(\frac{1+u}{1-u}\right)-\theta_c u. \tag{4.6}$$

We derive from (4.6) that the roots of $F'(u)$ are $\pm\beta$, where the positive root is given by

$$\frac{1}{2\beta}\ln\frac{1+\beta}{1-\beta}=\frac{\theta_c}{\theta}. \tag{4.7}$$

Hence, the extreme points $\pm\alpha$ of $F'(u)$ are given by

$$\alpha=\sqrt{1-\frac{\theta}{\theta_c}}=\sqrt{1-\frac{2\beta}{\ln\frac{1+\beta}{1-\beta}}}. \tag{4.8}$$

Just by Taylor expansion, it can be verified that

$$1-\frac{2s}{\ln\frac{1+s}{1-s}}<s^2,\quad \forall s\in(0,1). \tag{4.9}$$

Consequently, we have $\alpha<\beta$. A sketch of $f(x)=F'(x)$ is plotted in Figure 4.1. From

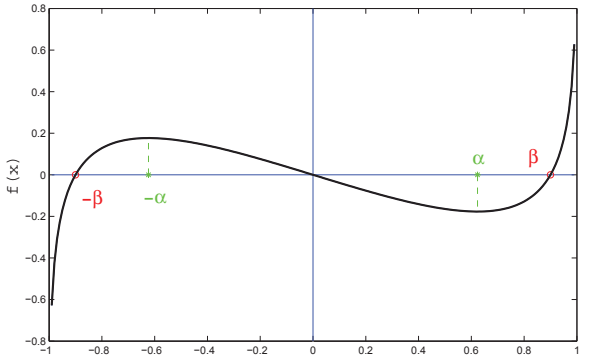

FIG. 4.1. *A sketch of* $f(x)=F'(x)$.

this figure, it is obvious that the logarithmic function $F(u)$ defined in (4.4) satisfies (1.5) and (1.6), and $M(u)$ given as (4.5) satisfies condition (1.7). Hence, the continuum Allen–Cahn model has maximum principle for these settings. It is reasonable to consider the numerical maximum principle:

COROLLARY 4.2. *Assume* $\max_{\boldsymbol{x}\in\bar{\Omega}}|u_0(\boldsymbol{x})|\le\beta$. *Then the fully discrete scheme* (3.6), *with the logarithmic free energy* (4.4) *and the degenerated nonlinear mobility* (4.5), *preserves the maximum principle in the sense that* $\|U^n\|_\infty\le\beta$ *for all* $n\ge0$ *provided that*

$$0<\tau\le\frac{\epsilon}{D(\theta-(1-3\beta^2)\theta_c)}; \tag{4.10}$$

and the stabilized fully discrete scheme (3.7) *with* (4.4)–(4.5) *preserves the maximum principle in the sense that* $\|U^n\|_\infty\le\beta$ *provided*

$$\frac{1}{\tau}+S\ge\frac{D(\theta-(1-3\beta^2)\theta_c)}{\epsilon}. \tag{4.11}$$

Proof. Since

$$M'(u) = -2Du, \quad F''(u) = \frac{\theta}{1-u^2} - \theta_c, \tag{4.12}$$

the condition (2.5) is equivalent to

$$\tau \max_{u\in[-\beta,\beta]} (\theta - \theta_c + 3\theta_c u^2 - 2\theta u \ln\frac{1+u}{1-u}) \le \frac{\epsilon}{D}. \tag{4.13}$$

It is nontrivial and not necessary to get the analytical maximum value in the above inequality, so we just offer a sufficient condition here.

It is observed that $u\ln\frac{1+u}{1-u}$ is nonnegative for $u\in(-1,1)$. This implies a sufficient condition for (4.13) as

$$\tau \max_{u\in[-\beta,\beta]} (\theta - \theta_c + 3\theta_c u^2) \le \frac{\epsilon}{D}. \tag{4.14}$$

Furthermore, it follows from (4.7) and (4.9) that

$$\theta > (1-\beta^2)\theta_c,$$

which leads to

$$\max_{u\in[-\beta,\beta]} (\theta - \theta_c + 3\theta_c u^2) = \theta - (1-3\beta^2)\theta_c > 0,$$

due to $\beta<1$. Combining above inequalities yields the desired result (4.10). The other case can be proved similarly. ∎

REMARK 4.3. Note that most existing works on the Allen–Cahn equation with logarithmic free energy assume that the numerical solution satisfies $-1<u<1$ to avoid singularity. While in this work, we established a discrete maximum principle which ensures that $|u|\le\beta<1$.

5. Error analysis

While it is relatively easy to establish some stability results for numerical schemes to the Allen–Cahn type equations, it is highly non-trivial to derive error estimates in the case with nonlinear degenerated mobility. In this section, we shall make use of the discrete maximum principle to carry out an error analysis for the fully discrete semi-implicit schemes in the maximum norm.

We consider the first scheme (3.6), which can be concisely rewritten as (with $n+1$ replaced by n)

$$\big(I - \tau\Lambda_1^n A_v - \tau\epsilon\Lambda_2^{n-1}(U^{n-1})D_h\big)U^n = U^{n-1} - \frac{\tau}{\epsilon}\Lambda_2^{n-1}(U^{n-1})F'(U^{n-1}), \tag{5.1}$$

where Λ_1^n and Λ_2^{n-1} are defined by (3.5). The error E^n is defined as

$$E^n = U(t_n) - U^n, \tag{5.2}$$

where $U(t_n)$ is the vector consisting of values of the exact solution of (1.1)–(1.2) at the grid points. We define the local truncation error T^n for the scheme (5.1) by

$$T^n = \Big(I - \tau\Lambda_1^n A_v - \tau\epsilon\Lambda_2^{n-1}(U(t_{n-1}))D_h\Big)U(t_n)$$

$$-\Big(U(t_{n-1})-\frac{\tau}{\epsilon}\Lambda_2^{n-1}(U(t_{n-1}))F'(U(t_{n-1})\Big). \tag{5.3}$$

Assuming that the exact solution $U(t)$ is sufficiently smooth, it is easy to check that

$$\|T^j\|_\infty \le c\tau\eta \quad \text{for} \quad j\le n, \tag{5.4}$$

where $\eta=\tau+h$ and $c=c(t_n)$ is a positive function of t_n, which may depend on $U(t)$ but not on τ or h. Denote

$$S_\beta^N=\{\boldsymbol{x}\in\mathbb{R}^N:\|\boldsymbol{x}\|_\infty\le\beta\}. \tag{5.5}$$

With the conditions (1.5)–(1.7), it has already shown that U^n (numerical maximum principle) and $U(t_n)$ (continuum maximum principle) both belong to S_β^N. With the help of establishing numerical maximum principle and existing continuum maximum principle, we can further show that there exist $\kappa_i>0$ $(1\le i\le 4)$ such that for any $\boldsymbol{p},\boldsymbol{q}\in S_\beta^N$

$$\|\Lambda_2(\boldsymbol{p})-\Lambda_2(\boldsymbol{q})\|_\infty\le\kappa_1\|\boldsymbol{p}-\boldsymbol{q}\|_\infty,\quad \|F'(\boldsymbol{p})-F'(\boldsymbol{q})\|_\infty\le\kappa_2\|\boldsymbol{p}-\boldsymbol{q}\|_\infty, \tag{5.6}$$

$$\|\Lambda_2(\boldsymbol{p})\|_\infty\le\kappa_3,\quad \|F'(\boldsymbol{p})\|_\infty\le\kappa_4. \tag{5.7}$$

Consider the case of Section 4.1, i.e., $M(u)=1$ and $F(u)=\frac{1}{4}(u^2-1)^2$. In this polynomial free energy case, we can verify that

$$\kappa_1=1,\quad \kappa_2=2,\quad \kappa_3=1,\quad \text{and}\quad \kappa_4=\frac{2}{3\sqrt{3}}.$$

For the case of Section 4.2, i.e., $F(u)$ and $M(u)$ given by (4.4) and (4.5), we can verify that

$$\kappa_1=2\beta D,\quad \kappa_2=\frac{\theta}{1-\beta^2}-\theta_c,\quad \kappa_3=D,\quad \text{and}\quad \kappa_4=F'(-\alpha),$$

where α, β, and D are given in (4.8), (4.7), and (4.5), respectively. It is noted that these constants are all independent of the mesh sizes.

THEOREM 5.1. *Assume that the solution of* (1.1)–(1.2) *is sufficiently smooth and* $\max_{\boldsymbol{x}\in\bar\Omega}|u_0(\boldsymbol{x})|\le\beta$. *Then we have the following error estimate for the scheme (5.1)*

$$\|E^n\|_\infty\le e^{\kappa t_n}\left(\|E^0\|_\infty+ct_n(\tau+h)\right), \tag{5.8}$$

where E^n *is defined by* (5.2) *and*

$$\kappa=\epsilon\beta\kappa_1+(\kappa_1\kappa_4+\kappa_2\kappa_3)/\epsilon, \tag{5.9}$$

provided that τ *satisfies (2.5).*

Proof. Subtracting (5.1) from (5.3) gives

$$\begin{aligned}
&\left(I-\tau\Lambda_1^nA_v-\tau\epsilon\Lambda_2^{n-1}(U^{n-1})D_h\right)E^n\\
&=E^{n-1}-\tau\epsilon\left(\Lambda_2^{n-1}(U^{n-1})-\Lambda_2^{n-1}(U(t_{n-1}))\right)U(t_{n-1})\\
&\quad-\tau\frac{1}{\epsilon}\left(\Lambda_2^{n-1}(U(t_{n-1}))F'(U(t_{n-1}))-\Lambda_2^{n-1}(U^{n-1})F'(U^{n-1})\right)+T^n\\
&=:E^{n-1}+S_{\mathrm{I}}^n+S_{\mathrm{II}}^n+T^n,
\end{aligned} \tag{5.10}$$

which yields

$$E^n = (I - G^{n-1})^{-1}(E^{n-1} + S_{\mathrm{I}}^n + S_{\mathrm{II}}^n + T^n), \tag{5.11}$$

where G^{n-1} is defined in (3.15). By (3.18) and (5.4), we have

$$\|E^n\|_\infty \le \|E^{n-1}\|_\infty + \|S_{\mathrm{I}}\|_\infty + \|S_{\mathrm{II}}\|_\infty + c\tau\eta. \tag{5.12}$$

It follows from (5.6) and (5.7) that

$$\|S_{\mathrm{I}}^n\|_\infty \le \tau\epsilon\beta\kappa_1\|E^{n-1}\|_\infty, \tag{5.13}$$

$$\begin{aligned}\|S_{\mathrm{II}}^n\|_\infty &= \tau\frac{1}{\epsilon}\Big\| \left(\Lambda_2^{n-1}(U^{n-1}) - \Lambda_2^{n-1}(U(t_{n-1}))\right) F'(U^{n-1}) \\ &\qquad + \Lambda_2^{n-1}(U(t_{n-1}))\left(F'(U^{n-1}) - F'(U(t_{n-1}))\right)\Big\|_\infty \\ &\le \tau\frac{\kappa_1\kappa_4 + \kappa_2\kappa_3}{\epsilon}\|E^{n-1}\|_\infty. \end{aligned} \tag{5.14}$$

Combining (5.13) and (5.14), we find from (5.12) that

$$\|E^n\|_\infty \le (1+\kappa\tau)\|E^{n-1}\|_\infty + c\tau\eta, \tag{5.15}$$

where κ is defined by (5.9). The above Gronwall-type inequality gives the desired result (5.8). ∎

Next, we will study the error estimate for the stabilized version of scheme (5.1) as

$$\Big((1+S\tau)I - \tau\Lambda_1^n A_v - \tau\epsilon\Lambda_2^{n-1}(U^{n-1})D_h\Big)U^n = (1+S\tau)U^{n-1} - \frac{\tau}{\epsilon}\Lambda_2^{n-1}(U^{n-1})F'(U^{n-1}). \tag{5.16}$$

Similarly, we define the truncation error for the above scheme as

$$\begin{aligned} T_S^n = &\Big((1+S\tau)I - \tau\Lambda_1^n A_v - \tau\epsilon\Lambda_2^{n-1}(U(t_{n-1}))D_h\Big)U(t_n) \\ &- \Big((1+S\tau)U(t_{n-1}) - \frac{\tau}{\epsilon}\Lambda_2^{n-1}(U(t_{n-1}))F'(U(t_{n-1}))\Big). \end{aligned} \tag{5.17}$$

Under the consistency assumption similar to (5.4), i.e.,

$$\|T^j\|_\infty \le c_s\tau\eta \quad \text{for} \quad j \le n, \tag{5.18}$$

and the same definitions for parameters κ_1, κ_2, κ_3, and κ_4 as in (5.6) and (5.7), we have the following error estimate for the stabilized scheme.

COROLLARY 5.2. *Assume that the solution of* (1.1)-(1.2) *is sufficiently smooth and* $\max_{\boldsymbol{x}\in\bar{\Omega}}|u_0(\boldsymbol{x})| \le \beta$. *Then we have the following error estimate for the scheme (5.16)*

$$\|E^n\|_\infty \le e^{\kappa t_n}\left(\|E^0\|_\infty + c_s t_n(\tau + h)\right) \tag{5.19}$$

where κ *is defined by* (5.9), *provided that* τ *satisfies* (2.16).

6. Numerical results

In this section, we present some numerical experiments to verify theoretical results obtained in the previous sections. Since the polynomial free energy has been studied in [17], we will only focus on the more difficult case with logarithmic free energy below.

EXAMPLE 6.1. We first consider the one-dimensional Allen–Cahn equation with logarithmic free energy (4.4) and nonlinear mobility (4.5) subject to the homogeneous Dirichlet boundary condition with the initial value $u_0(x) = -0.9\sin(50x)$. The velocity field is given as $v(x,t) = e^t \sin(x)$.

We take $\epsilon = 0.01, D = 1, \beta = 0.94$ assume the computation domain to be $[0, 2\pi)$. An equidistant mesh in space with $N = 200$ is used. Note that u_0 takes the value -0.9 and 0.9 at nodes alternately. Numerical results with different time step τ and stabilization parameter S are presented in Figure 6.1.

We denote the constants in (4.10) and (4.11) by

$$M_{\text{tol}} = \frac{D(\theta - (1-3\beta^2)\theta_c)}{\epsilon}, \quad t_{\text{tol}} = \frac{\epsilon}{D(\theta - (1-3\beta^2)\theta_c)}. \tag{6.1}$$

For Example 6.1, $t_{\text{tol}} = 0.046$. First, we set the stabilization parameter S to be 0, i.e., we use the standard implicit-explicit scheme (3.6). The maximum value of the numerical solutions at different time is shown in the left part of Figure 6.1. It is observed that when $\tau = t_{\text{tol}}$ and $\tau = 2.5t_{\text{tol}}$ the discrete maximum principle is preserved. However, if the time step $\tau = 5t_{\text{tol}}$, the violation of the maximum principle occur. These results indicate that (4.10) in Corollary 4.2 is a sufficient but not a necessary condition for preserving the discrete maximum principle. Figure 6.1 also shows the results given by using $S = 0.1M_{\text{tol}}$. In this case, it is seen that the scheme preserves the discrete maximum principle even when time step $\tau = 10t_{\text{tol}}$. With this large time step, non-stabilized schemes will blow up almost immediately. Hence, the stabilized scheme (3.7) allows much larger time steps with reasonable size of S.

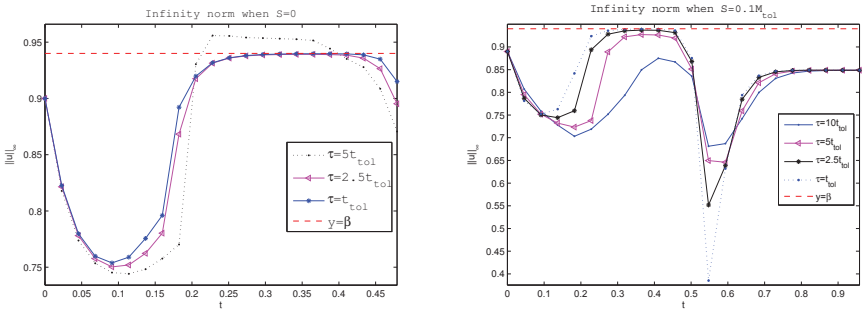

FIG. 6.1. *Example 6.1: maximum values with $S = 0$ (left) and $S = 0.1M_{\text{tol}}$ (right) using different time steps.*

EXAMPLE 6.2. Consider the 2D Allen–Cahn equation with logarithmic free energy (4.4) and nonlinear mobility (4.5) subjected to the homogeneous Dirichlet boundary condition with the following random initial value

$$u_0(x,y) = 0.05(2 \cdot \text{rand} - 1), \tag{6.2}$$

where 'rand' is a random number in $[0,1]$. The components of $\boldsymbol{v}$ are those for the clockwise rotational velocity field of the form $v_1(x,y,t) = y - \pi$ and $v_2(x,y,t) = \pi - x$.

We take the parameters $\epsilon = 0.1$, $D = 1$ and the computation domain to be $[0, 2\pi] \times [0, 2\pi]$. The mesh in space is fixed with $N_x = N_y = 100$, and we set $\beta = 0.95$. Then we see $t_{\text{tol}} = 0.045$. In this example, we take $S = 0$ and time step $\tau = 0.04$ which is smaller than

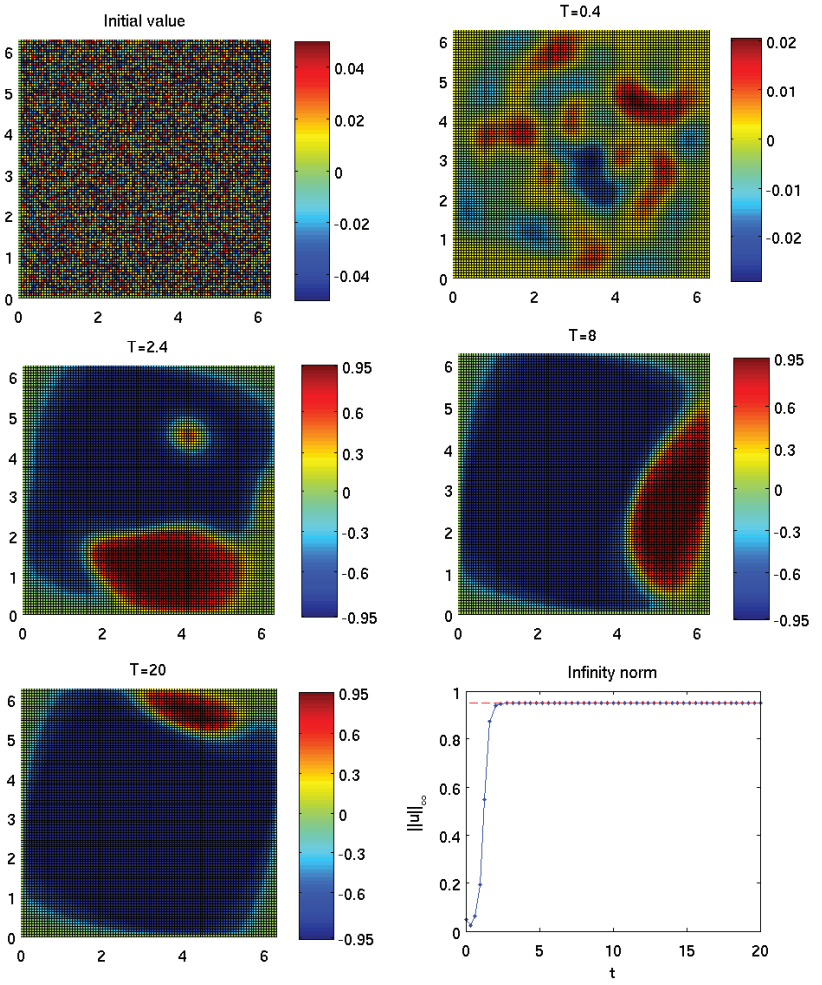

FIG. 6.2. *Example 6.2: solution evolution and maximum values.*

t_{tol}. Evolutions and maximum values of numerical solutions are presented in Figure 6.2. It is observed in the last sub-figure that the discrete maximum principle are indeed well preserved. Moreover, the ordering and coarsening phenomena as well as the rotation effect due to the advection term are well observed.

The last example aims to emphasize the significant impact of the stabilized scheme in the long time simulations, especially after being equipped with some time-stepping adaptivity strategy. To this end, we consider a simple case with zero velocity field and constant mobility D.

EXAMPLE 6.3. Consider the 2D Allen–Cahn equation with zero velocity field and constant mobility D in $[0,2\pi]\times[0,2\pi]$ with logarithmic free energy (4.4) subject to the periodic boundary condition. The random initial value (6.2) is taken.

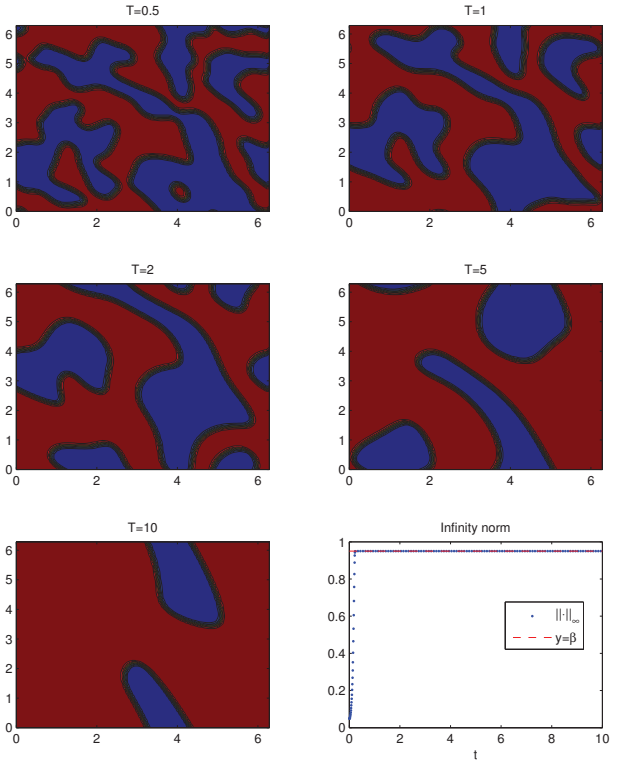

FIG. 6.3. *Example 6.3: solution evolution and maximum value obtained by non-stabilized scheme with fine time-step* $\tau = 10^{-4}$.

It is noted that due to the periodic boundary condition fast solvers are used in the computation. In this example, we take the parameters $\epsilon = 0.04$ and $D = 2$. Same as in Example 2, the mesh in space is fixed with $N_x = N_y = 100$, and we set $\beta = 0.95$. In this case, the time step size constraint (2.16) is equivalent to

$$\frac{1}{\tau} + S \geq \frac{D}{\epsilon}\left(\frac{\theta}{1-\beta^2} - \theta_c\right) =: M_{\text{tol}}. \tag{6.3}$$

The standard scheme require time step smaller than $t_{\text{tol}} = \frac{1}{M_{\text{tol}}} = 0.0046$.

First, we obtain the reference solution by the non-stabilized scheme with very small uniform time step $\tau = 10^{-4}$. The fine time-step solution is shown in Figure 6.3. We then implement the stabilized scheme together with an adaptive time-stepping strategy proposed by Gomez and Hughes [12]. The main idea is to update the time step size by using the formula

$$A_{\text{dp}}(e,\tau) = \rho\left(\frac{\text{tol}}{e}\right)^{1/2}\tau, \tag{6.4}$$

where ρ is a default safety coefficient, tol is a reference tolerance, and e is the relative error at each time level. Following [12], we choose $\rho = 0.9$ and $\text{tol} = 10^{-3}$. The minimum

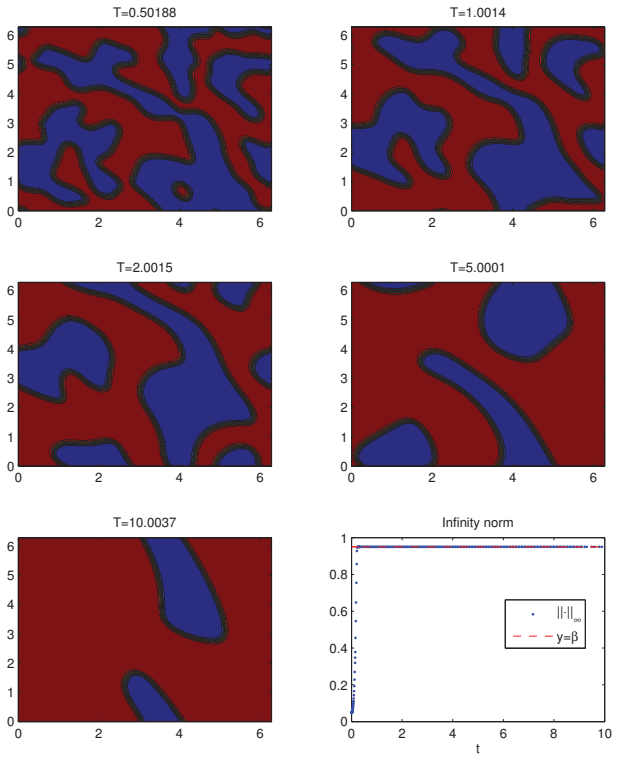

FIG. 6.4. *Example 6.3: solution evolution and maximum value obtained by using the stabilized scheme with adaptive time-stepping algorithm.*

and maximum time steps are taken as $\tau_{\min} = 10^{-4}$ and $\tau_{\max} = 10^{-1}$, respectively, with a ratio of 100. The initial stabilizing parameter S is taken as 0.

Note that in our algorithm the stabilized parameter S is chosen adaptively based on (6.3). By doing this, the discrete maximum principle will be preserved, since $S \geq M_{\text{tol}} - \frac{1}{\tau}$ is a sufficient condition to guarantee the maximum principle. We emphasize again preserving the maximum principle is extremely important for the logarithmic free energy (resp. nonlinear mobility), as the failure of the discrete maximum principle will lead to meaningless definition of the energy functional (resp. negative mobility value). (4.4).

Snapshots of phase evolution and time history of maximum values for numerical solutions are shown in Figure 6.4, and the adaptive time steps and stabilized parameters are shown in Figure 6.5. It is observed that the adaptive-time solutions given in Figure 6.4 are in good agreement with the reference solutions presented in Figure 6.3. It is seen from Figure 6.5 (a) that the time step progressively increases based on the energy evolution of the solution. When the coarsening becomes dominant (e.g., $t > 1$), the time steps become larger, which shows that the time adaptivity based on the stabilized scheme works well for the Allen–Cahn problem. Figure 6.5 (b) shows the variation of the stabilization parameters S. It is observed that S increases significantly at $T \approx 9$ after

Algorithm 1 Time step and stabilized coefficient adaptive procedure

Given: U^n, τ_n and stabilized parameter S_n.

Step 1. Compute U_{FE}^{n+1} by the forward Euler method with τ_n.

Step 2. Compute U^{n+1} by the the stabilized scheme method with τ_n and S_n.

Step 3. Calculate $e_{n+1} = \frac{||U_{FE}^{n+1} - U^{n+1}||}{||U^{n+1}||}$

Step 4. **if** $e_{n+1} > \text{tol}$, **then**

Recalculate time step $\tau_n \leftarrow \min\{A_{\text{dp}}(e_{n+1}, \tau_n), \tau_{\max}\}$ and stabilized parameter $S_n \leftarrow \min\{0, M_{\text{tol}} - \frac{1}{\tau_n}\}$

Step 5. **goto** Step 1

Step 6. **else**

Update time step $\tau_{n+1} \leftarrow \min\{A_{\text{dp}}(e_{n+1}, \tau_n), \tau_{\max}\}$ and stabilized parameter $S_{n+1} \leftarrow \min\{0, M_{\text{tol}} - \frac{1}{\tau_{n+1}}\}$

Step 7. **endif**

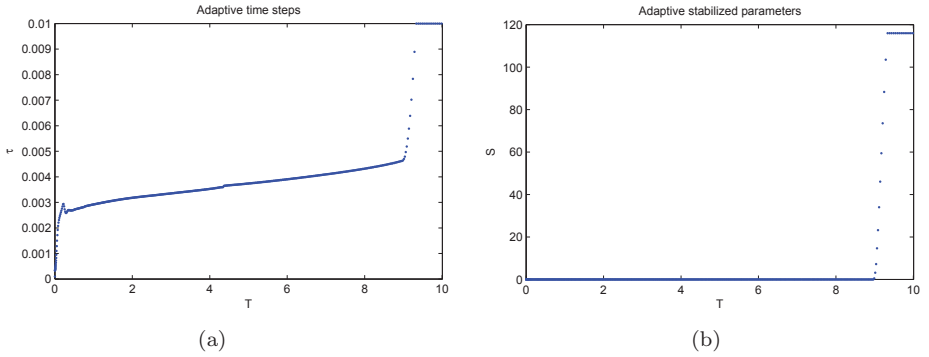

(a) (b)

FIG. 6.5. *(a) adaptive time steps and (b) adaptive stabilized parameters.*

which the time step is taken as $\tau_{\max}$. Due to the use of large stabilization parameter, the effective time step is smaller than the time step used in the stabilized scheme so it results in a slight lagging effect which can be seen by comparing Figure 6.5 to Figure 6.4. This effect can be reduced by restricting the stabilization parameter S and/or $\tau_{\max}$ to a smaller range.

7. Conclusions

We considered in this paper numerical approximations of the generalized Allen–Cahn equations, which include cases with logarithmic free energy, nonlinear degenerated mobility, and/or additional advection term. We studied the stability of the scheme with first-order semi-implicit treatment in time (with or without a stabilizing term) and the central finite difference for the diffusion term and upwind scheme for the advection term in space. We proved that this conventional scheme preserves the discrete maximum principle under some reasonable time step constraint. We also proved that adding a stabilizing term can significantly increase the allowable time step.

We presented numerical examples using the stabilized scheme together with an adaptive strategy to select the stabilized parameters. The numerical results indicate

the effectiveness of the proposed approach, which also verify the theoretical results obtained in this work.

REFERENCES

[1] S.M. Allen and J.W. Cahn, *A microscopic theory for antiphase boundary motion and its application to antiphase domain coarsening*, Acta Metall, 27, 1085–1095, 1979.

[2] Michal Benes, V. Chalupecky, and K. Mikula, *Geometrical image segmentation by the Allen–Cahn equation*, Applied Numerical Mathematics, 51, 187–205, 2004.

[3] L. Cherfils, A. Miranville, and S. Zelik, *The Cahn–Hilliard equation with logarithmic potentials*, Milan Journal of Mathematics, 79(2), 561–596, 2011.

[4] M.I.M. Copetti and C.M. Elliott, *Numerical analysis of the Cahn–Hilliard equation with a logarithmic free energy*, Numerische Mathematik, 63(1), 39–65, 1992.

[5] Q. Du and R.A. Nicolaides, *Numerical analysis of a continuum model of phase transition*, SIAM J. Numer. Anal., 28, 1310–1322, 1991.

[6] C.M. Elliott and A.M. Stuart, *The global dynamics of discrete semilinear parabolic equations*, SIAM J. Numer. Anal., 30(6), 1622–1663, 1993.

[7] D.J. Eyre, *An unconditionally stable one-step scheme for gradient systems*, June 1998, unpublished, http://www.math.utah.edu/eyre/research/methods/stable.ps.

[8] X. Feng and A. Prohl, *Numerical analysis of the Allen–Cahn equation and approximation for mean curvature flows*, Numerische Mathematik, 94(1), 33–65 2003.

[9] X. Feng, H. Song, T. Tang, and J. Yang, *Nonlinearly stable implicit-explicit methods for the Allen–Cahn equation*, Inverse Problems and Imaging, 7, 679–695, 2013.

[10] X. Feng, T. Tang, and J. Yang, *Stabilized Crank–Nicolson/Adams–Bashforth schemes for phase field models*, East Asian Journal on Applied Mathematics, 3, 59–80, 2013.

[11] X. Feng, T. Tang, and J. Yang, *Long time numerical simulations for phase-field problems using p-adaptive spectral deferred correction methods*, SIAM J. Sci. Comput., 37(1), A271–A294, 2015.

[12] H. Gomez and T.J.R. Hughes, *Provably unconditionally stable, second-order time-accurate, mixed variational methods for phase-field models*, J. Comput. Phys., 230, 5310–5327, 2011.

[13] T. Ilmanen, *Convergence of the Allen–Cahn equation to Brakke's motion by mean curvature*, J. Differential Geom., 38(2), 417–461, 1993.

[14] Junseok Kim, *Phase-field models for multi-component fluid flows*, Commun. Comput. Phys., 12, 613–661, 2012.

[15] J. Shen and X. Yang, *Numerical approximations of Allen–Cahn and Cahn–Hilliard equations*, Discret. Contin. Dyn. Syst., 28, 1669–1691, 2010.

[16] J. Shen and X. Yang, *A phase-field model and its numerical approximation for two-phase incompressible flows with different densities and viscosities*, SIAM J. Sci. Comput., 32, 1159–1179, 2010.

[17] T. Tang and J. Yang, *Implicit-explicit scheme for the Allen–Cahn equation preserves the maximum principle*, J. of Comp. Mathematics, to appear, 2013.

[18] Y. Xia, Y. Xu, and C.-W. Shu, *Local discontinuous Galerkin methods for the Cahn–Hilliard type equations*, J. Comput. Phys., 227, 472–491, 2007.

[19] X. Yang, *Error analysis of stabilized semi-implicit method of Allen–Cahn equations*, Discrete Contin. Dyn. Syst. Ser. B, 11(4), 1057–1070, 2009.

[20] J. Zhang and Q. Du, *Numerical studies of discrete approximations to the Allen–Cahn equation in the sharp interface limit*, SIAM J. Sci. Comput., 31(4), 3042–3063, 2009.